Correcting for instrumentation with corrugated fiberboard edgewise crush test theory

Thomas J. Urbanik

Research general engineer, USDA Forest Service, Forest Products Laboratory, One Gifford Pinchot Dr., Madison, Wis. 53705-2398

ABSTRACT *A theory of corrugated fiberboard short column failure by buckling is incorporated within a semiempirical model that further accounts for postbuckling behavior. A theory of metal postbuckling failure is applied to paper to specifically derive a set of postbuckling constants, $\theta_0, \theta_1, \theta_2$. Values for these constants differ with each user's unique testing methods, but the constants can be used to correct for instrumentation differences. A set of equations results in a form that can be used to predict the elastic, inelastic, or combined failure modes and can thereby confirm or refute the accuracy of the test methods. Software based on this theory is being developed for use by packaging engineers. It is intended as easy-to-use software for determining the optimum design of corrugated containers.*

KEYWORDS
Analysis
Buckling
Corrugated boards
Deformation
Strain
Strength properties
Stress
Testing

Knowing how to predict the edgewise compressive strength (i.e., the short column strength) of corrugated fiberboard has important implications in evaluating the linerboard and corrugating medium material. The problem is complicated by the wide variety of testing methods used to measure basic paper properties and fiberboard strength. At least two test methods, the ring crush test (1) and the short span test (2), are popular for determining paper strength. Koran and Kamdem (3) have examined five different methods for measuring paper stiffness.

Further alternatives arise in opting for a corrugated fiberboard strength test. Stott (4) advocates a method, known as FEFCO (European Federation of Corrugated Board Manufacturers), based on an assessment of various methods compared in a worldwide interlaboratory study. Koning (5) challenges Stott in favor of test methods known to cause localized failure, to be consistent with buckling theory.

A revision of Rule 41 (6) that would rely on edgewise compressive strength determined by the TAPPI method (7) is under consideration (8). Concurrently, the American Society for Testing and Materials (ASTM) is considering a performance standard (9) based on its own strength test (10).

The paper industry and standards organizations will probably never reach a worldwide consensus on which paper tests and fiberboard tests work best. The objective here is to propose a way to reconcile the controversies surrounding the lack of agreement. Our solution, based on mechanistic principles, can have a favorable impact on the criteria for determining a set of fiberboard manufacturing strength grades, can unify the results from alternative testing methods, and ultimately can affect the use of over 20 million metric tons of fiber used annually in the United States.

Short column failure mechanism

A short column of corrugated fiberboard can be considered as an assembly of long thin microplates joined at the corrugation glue lines and loaded in the plate-axis direction. Here, we consider the failure mechanism precipitated by localized buckling followed by a measurement-dependent postbuckling deformation phenomenon **(Fig. 1).** We consider failure to coincide with the strength measured under edgewise compression. Plate elements can buckle elastically and can then sustain additional loading up to failure; or they can buckle inelastically, followed by continuous deformation, but with no additional loading.

The short-column apparent failure strain (deformation per specimen gauge length) can significantly exceed the compression failure strain of the microplate elements. Deformations have been observed (11) around 2%, far beyond the typical strains of

1. Progression of localized buckling in corrugated fiberboard short columns from a stable configuration to a postbuckled failure mode. In A, the facings buckle first, in B, the core buckles first Compression is between two glass platens with a view through the flutes.

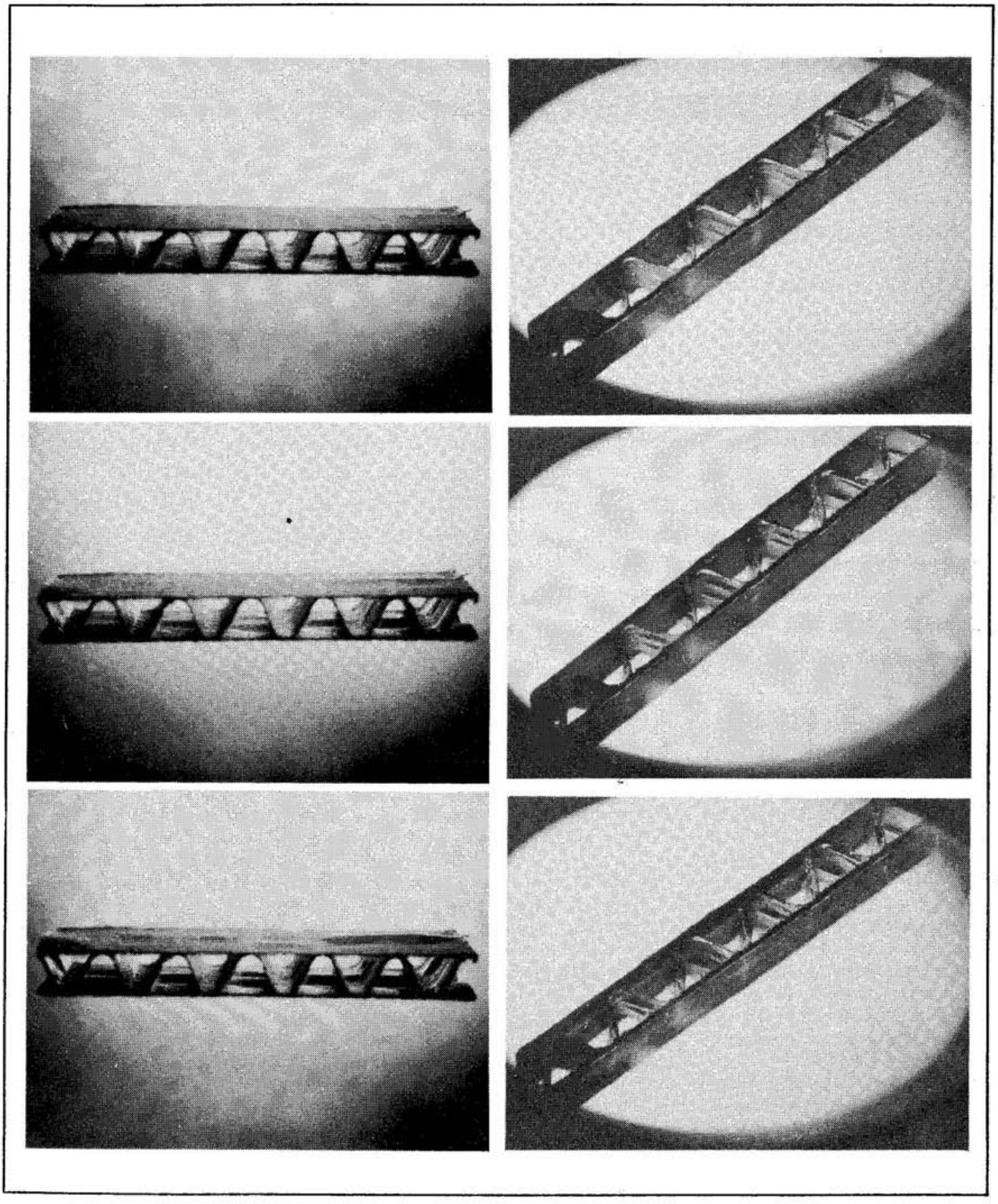

0.5% measured at uniaxial compression failure for the individual components (12).

Use of buckling theory

In the failure of metal plate structures, component plates continue to deform and redistribute their loads after buckling (13). An adaptation of

2. Comparison between paper stress–strain curve and short column apparent stress–strain curve up to elastic failure. Below σ_{cr}, it is assumed in buckling theory that deformation occurs along the stress–strain curve. From σ_{cr} to σ_f, postbuckling theory accounts for deformation along the dashed curve. Inelastic failure gives $\sigma_f = \sigma_{cr}$.

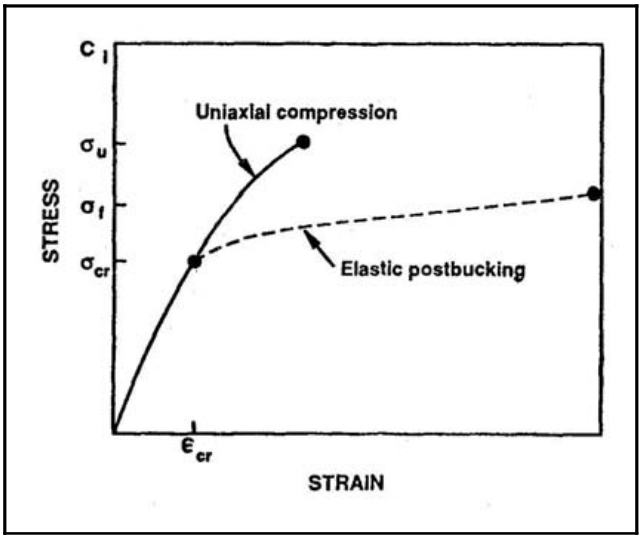

3. Comparison of Eq. 3 for $N = 0.2$ and $N = 2$ with Eqs. 1 and 2. Around $N = 10$, Eq. 3 becomes indistinguishable from Eqs. 1 and 2.

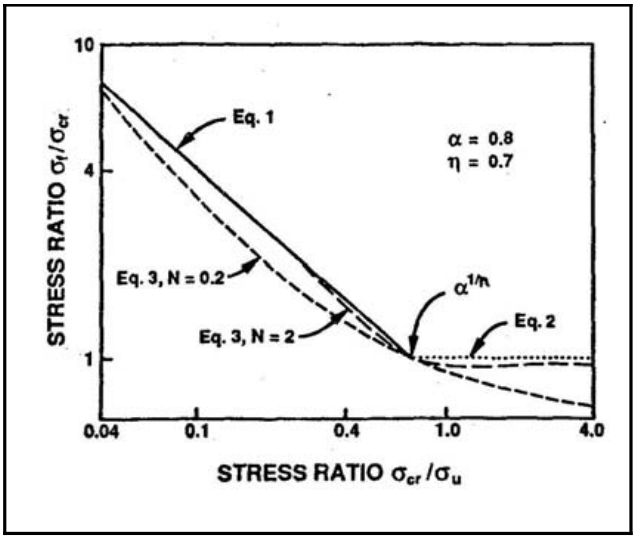

load distribution concepts (14) relates the average stress σ_f across the plate cross section at failure to the average stress σ_{cr} at its predicted critical buckling load and to the material stress σ_u at the ultimate strength under uniaxial loading with the semiempirical relationships

$$\sigma_f/\sigma_{cr} = \alpha\,(\sigma_u/\sigma_{cr})^{\eta} \quad \text{for } \sigma_{cr} \le \alpha^{1/\eta}\,\sigma_u \tag{1}$$

and

$$\sigma_f/\sigma_{cr} = 1 \quad \text{for } \sigma_{cr} > \alpha^{1/\eta}\,\sigma_u \tag{2}$$

where a and η are postbuckling constants. Stress levels **(Fig. 2)** are considered as average values across the plate cross section.

Relatively thin plates would fail by elastic buckling according to Eq. 1. Relatively thick or stiff plates would fail by plastic buckling according to Eq. 2. Beyond its application to metal plates, Eq. 1 was also applied to paper to derive McKee's box compression formula (15), assuming only elastic buckling.

In our previous research, we derived the theory for the buckling, first of plates (16) and then of plate structures (17), appropriate for paper. Basic inputs for analyzing paperboard short columns include the paper compression stress–strain properties prior to corrugating. The output is the short column critical strain ϵ_{cr}, from which a value of σ_{cr} is calculated for each component from its stress–strain relationship. To account for high deformations in short column failure, our approach here is to treat the microplate linerboard and corrugating medium elements as being further subject to a combination of elastic and inelastic buckling and to assume that metal plastic buckling theory can characterize paper inelastic buckling.

One difficulty in fitting Eqs. 1 and 2 to combined failure mode data is that the value of $\alpha^{1/\eta}$ must be known before segregating the data. To resolve this, we introduce the continuous relationship

$$\sigma_f/\sigma_{cr} = 1 + X\,[(\tanh NX)/2 + (1/2)] \tag{3}$$

$$X = \alpha\,(\sigma_u/\sigma_{cr})^{\eta} - 1 \tag{4}$$

where the constant N is chosen as an arbitrarily large number. As N approaches infinity, Eq. 3 approaches the form of Eq. 1 when $X > 0$ and the form of Eq. 2 when $X < 0$ **(Fig. 3).** Equation 3 is empirical but has been found to work well in matching our buckling theory to data.

Method

To adapt our buckling theory to commercial instruments, we first introduce the postbuckling constant θ_0 that corrects the paper stress–strain properties for a proportionality error among alternative instruments. Two other constants, θ_1 and θ_2, account for the postbuckling deformation that depends on the edgewise compression test (ECT) apparatus and its induced specimen loading edge stress. Constants θ_1 and θ_2 approximately correct for a material property offset from its true value and for nonlinear errors.

Correcting for paper property test methods

Material constants c_1 and c_2 of the relationship

$$\sigma\,(\epsilon) = c_1 \tanh\,[(c_2/c_1)\,\epsilon\,] \tag{5}$$

between stress σ and strain ϵ, proposed for the uniaxial compression of paper (18), can be determined from the curve-fitting procedure reported (19, 20) using lateral support test data (12). Constant c_2 is taken from the initial slope of the stress–strain curve, and c_1 is taken from a horizontal asymptote slightly higher than the material stress σ_u at the ultimate load (Fig. 2). Alternatively, c_2 can be independently determined from an extension test of unit width stiffness E_u, and σ_u can be determined from a compression test of unit width strength S_u. The product $(\theta_0\,\sigma_u)$ can then be substituted for c_1 if

$$\theta_0 = c_1/\sigma_u \tag{6}$$

can be averaged from known lateral support data.

The accuracy of the material constants thus depends on how E_u and S_u

4. Form of the relationship between the stress ratio σ_f/σ_u and stiffness S for an individual plate according to Eq. 16. The value of $\hat{\sigma}$ in Eq. 16 is determined assuming $\nu = \nu' = 0.25$.

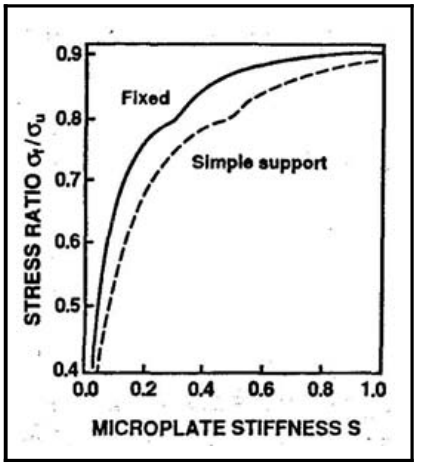

5. Comparison between the stress-strain curve constant c_1 and ultimate stress σ_u, in mega-Pascals. The line is the average given by $C_1 = 1.33\ \sigma_u$.

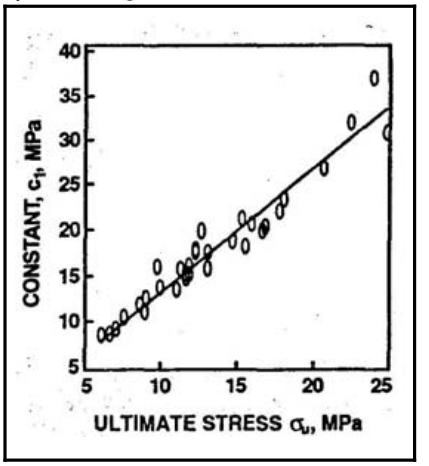

6. Comparison between the edgewise compressive strength of corrugated fiberboard predicted according to Eq. **18** and measured

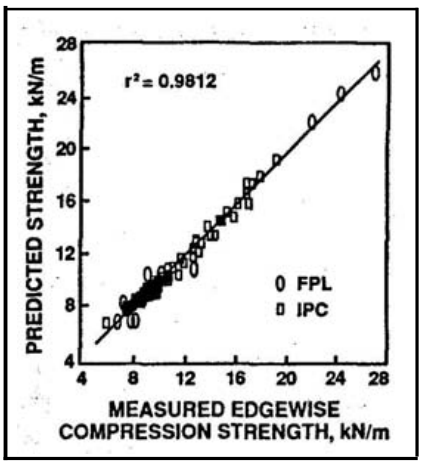

are measured and, further, on either measuring or calculating the material effective thickness (21, 22) defined as

$$t_e = (12\ EI_u/E_u)^{1/2} \tag{7}$$

where EI_u is unit width flexural stiffness.

Plate buckling stress σ_{cr} depends on stiffness. A dimensionless microplate stiffness S that characterizes the lateral stability of paper elements between corrugation glue lines and further incorporates θ_0 has the form derived earlier (16), given here by

$$S = [c_2/(\theta_0\sigma_u)]\,(t_e/w)^2\,(\nu'/\nu)^{1/2}$$
$$= [E_w/(\theta_0 S_u)]\,(t_e/w)^2\,(E_u'/E_u)^{1/2} \tag{8}$$

where ν is Poisson's ratio and w is the microplate width. Properties are associated with the loading direction except where the prime sign (') indicates the transverse direction. If the parameters defining S could be measured without error, then the value of θ_0 given by Eq. 6 could thus be substituted into Eq. 8. Otherwise, θ_0 becomes a function of the overall instrumentation proportionality error.

Given S for each plate and ϵ_{cr}, then a, is calculated in an earlier report (17) by first determining a dimensionless critical stress $\hat{\sigma}$ associated with each plate from

$$\hat{\sigma} = \tanh[(c_2/c_1)\,\epsilon_{cr}] \tag{9}$$

The accuracy of $\hat{\sigma}$ thus depends on the various test methods and material property correlations used to predict

I. Material test methods and substitutions for satisfying missing data

Material	Basis weight, g/m²	Paper test methods and substitutions: Thickness t_c	Thickness t_e	S_u	E_u CD	E_u MD	EI_u	Short column ECT method
FPL linerboard	126-451	DM	MM	LS	LS	LS	...	...
FPL medium	126-203	DM	MM	LS	LS	LS	...	...
FPL A-flute	...	...	...	...	...	...	...	RS
FPL C-flute	...	...	...	...	...	...	...	RS
IPC linerboard	137-437	DM	$\sqrt{12EI_u/E_u}$	MR	IT	IT	TS	...
IPC medium	84-268	DM	$a_0 + a_1 t_c$	MR	IT	CD E_u	...	...
IPC C-flute	...	...	...	...	...	...	...	TP

CD = cross direction. MD = machine direction. DM = dial micrometer (29). IT = Instron tension (25). LS = lateral support (12). MM = modified micrometer (21). MR = modified ring crush (1). RS = router shaped (27). TP = TAPPI T811 (7). TS = Taber stiffness (26).

the stress-strain curve. In applying **Eqs. 1-4** to paper data, the dependent and the independent variables become associated with various measurement errors. By incorporating θ_0 in the determination of

$$\sigma_{cr} = c_1\hat{\sigma} = \theta_0\,\sigma_u\hat{\sigma} \tag{10}$$

using Eq. 6, we provide a way to empirically correct for errors involving σ_u and σ_{cr}.

Correcting for ECT method

Our previous work (16) showed how $\hat{\sigma}$ varies with S for plates having simple or fixed ends. To further account for suspected postbuckling deformation, we apply Eqs. 1-3. Considering the case of elastic buckling first, substituting Eq. 10 into Eq. 1, and rearranging terms leads to the prediction of average failure stress:

$$\sigma_f = \alpha\theta_0^{1-\eta}\sigma_u\hat{\sigma}^{1-\eta} \tag{11}$$

To account for errors involving σ_f, we next define the paper postbuckling constants θ_1 and θ_2 in terms of θ_0, α, and η:

$$\theta_1 = \alpha\,\theta_0^{1-\eta} \tag{12}$$

$$\theta_2 = 1 - \eta \tag{13}$$

The result obtained from combining Eqs. 11-13 and rearranging terms is the nonlinear elastic postbuckling relationship:

$$\sigma_f = \theta_1\sigma_u\,\hat{\sigma}^{\theta_2} \tag{14}$$

$$\text{for } \hat{\sigma} \le (\theta_1/\theta_0)^{1/(1-\theta_2)}$$

Repeating the analysis using Eq. 2 for the case of inelastic buckling yields

$$\sigma_f = \theta_1 \sigma_u \hat{\sigma}^{\theta_2} \quad (15)$$

$$\text{for } \theta_1 = \theta_0 \text{ and } \theta_2 = 1$$

Then using Eq. 3 for elastic plus inelastic buckling yields

$$\sigma_f = \theta_0 \sigma_u \hat{\sigma} \{1 + X [(\tanh N X)/2 + 1/2]\} \quad (16)$$

$$\text{for } N >> 1$$

$$X = (\theta_1/\theta_2)\hat{\sigma}^{\theta_2 - 1} - 1 \quad (17)$$

Light grades of paper would be expected to buckle elastically according to Eq. 14. Heavier grades would buckle inelastically by Eq. 15. Equation 16 switches between the forms of Eqs. 14 and 15, depending on the value of X.

In Fig. 4, we extend the earlier results (16) to show how the microplate average failure stress would vary with S according to Eqs. 14–16. The knee in each curve corresponds to the transition from elastic to inelastic buckling when $X = 0$ in Eqs. 16 and 17. Curves of this form for each microplate can be summed to determine the short column strength. Varying θ_0 shifts the curves left and right to compensate for errors among the paper properties defining S. The values of θ_1 and θ_2 are functions of the ECT method and further correct for instrumentation offset and nonlinearities.

Evaluating postbuckling constants from data

The short column postbuckling strength P_f is the sum of loads due to each microplate according to

$$P_f/w_0 = \sum \sigma_f [\theta_0, \theta_1, \theta_2, \sigma_u t_c (w/w_0), \hat{\sigma}] \quad (18)$$

The value of w_0 is a unit structure width when characterizing periodic structures, or it can be set equal to 1 in applying our theory to discrete box structures. If data can be obtained for P_f as a function of σ_u and $\hat{\sigma}$, then constants θ_0, θ_1, θ_2 can be determined from a regression analysis incorporating Eqs. 16-18. The value of θ_0, used in calculating S, needs to agree with the value determined from Eq. 18.

The steps in determining θ_0, θ_1, θ_2 are:

1. Assume a value of θ_0.
2. Analyze a set of short columns.
3. From the results, create a database of P_f as a function of σ_u and $\hat{\sigma}$.
4. Fit Eq. 18 to the data.

If the new estimate of θ_0 matches the assumption, convergence is indicated. Otherwise, the assumed value of θ_0 must be updated, and the other steps must be repeated. The confidence intervals determined. for θ_0, θ_1, θ_2 indicate if the set of short columns failed by a combination of elastic and inelastic buckling according to Eq. **16** or if a simpler failure mechanism according to either Eq. **14** or **15** is sufficient.

Results

We have used our theory to successfully predict edgewise compressive strength from paper properties involving two independent data sets. Values of θ_0, θ_1, θ_2 for each data set correct for instrumentation differences and also for the effect of missing data.

For a previous Forest Products Laboratory (FPL) study (23), linerboard and corrugating medium papers were measured using lateral support (12) and effective thickness (21, 22) test methods that yielded all the properties needed to evaluate S. Components were converted into A- and C-flute corrugated boards at low speeds on an experimental corrugator. For another IPC study (formerly The Institute of Paper Chemistry, now The Institute of Paper Science and Technology) (24), linerboards were measured by alternative, yet still complete, methods using commercial instruments now specified as the ring crush (1), tension (25), and Taber stiffness (26) methods. Corrugating mediums were measured for only tension and strength properties. From these materials, C-flute boards were made on a production corrugator. Measurements of paper caliper t_c and flute profile calculations of w defined the structure geometry for edgewise compression strength calculations.

Dealing with missing data

Knowing any two of the properties te, E_u, and EI_u, the third can be determined from Eq. 7. Because the IPC corrugating medium data lacked sufficient information to determine t_e by definition, a correlation in terms oft, was substituted:

$$t_e = a_0 + a_1 t_c \quad (19)$$

We therefore relied on the FPL data to evaluate the regression constants $a_0 = 65.2$ mm and $a_1 = 1.12$. Another deficiency was not having machine. direction E_u data. Therefore the cross-direction values were used.

ECT methods

The databases further differ by the fiberboard ECT methods. Whereas in the FPL study a router-shaped specimen was used according to a procedure described by Koning (27), in the IPC study the researchers followed what is now a TAPPI method (7). These methods are equivalent for low-basis-weight materials; the router method gives higher strength values than the TAPPI method for materials of heavy basis weight. Table I summarizes the test methods and substitutions used to determine the various material properties.

FPL postbuckling constants

An initial estimate of $\theta_0 = 1.33$ was obtained from the average of c_1/σ_u (Fig. 5). We found that after repeatedly updating the estimate of θ_0 until convergence, the difference of fits between Eqs. 14 and 16 was insignificant. Because the data included only three high-strength short columns (Fig. 6), the difference betweenelastic and inelastic failure was not significantly detected. Therefore, Eq. 14 for the simpler elastic buckling was appropriate.

The final postbuckling constants were $\theta_0 = 1.33$, $\theta_1 = 0.837 \pm 0.0232$, and $\theta_2 = 0.384 \pm 0.159$. The tolerances given with θ_1 and θ_2 span the approximate 95% confidence intervals based on a linear hypothesis. The agreement between the postbuckling prediction of θ_0 with the value from Eq. 6 according to compression data supports the accuracy of the methods of Gunderson (12) and Setterholm (21) for measuring paper compression stress–strain properties.

IPC postbuckling constants

The final IPC postbuckling constants were $\theta_0 = 0.878 \pm 0.0160$, $\theta_1 = 0.780 \pm 0.0740$, and $\theta_2 = -0.244 \pm 0.00532$. In this second case, both elastic and inelastic failures were evident according to the significance of Eq. 16. Both

failure modes were expected, due to the planned combinations of low-basis-weight and high-basis-weight papers among the IPC data. The value of $\theta_0 = 0.878$, low compared with the FPL data, indicates that t_e, E_u, and/or E'_u were underestimated and/or that S_u and/or w were overestimated relative to the other properties.

The negative value of θ_2 predicts that σ_f decreases with an increasing $\hat{\sigma}_*$. This could result [as predicted by Whitsitt and Sprague (28)] from the high-basis-weight mediums having been more severely stressed and correspondingly degraded during corrugating, compared to the low-basis-weight mediums. A negative θ_2 also could have resulted from nonlinear ring crush errors with respect to basis weight or from the ECT method causing premature inelastic buckling for heavy-weight materials.

Predictions are compared with measurements for both data sets in Fig. 6. The average value found for θ_1 predicts that paper in a short column structure can carry up to 0.8 times its precorrugated strength, depending on its stiffness S.

Discussion: choosing the best tests

The results of our FPL and IPC analyses demonstrate that excellent ECT strength predictions are possible regardless of the paper and fiberboard test methods. A more complete critique of superior tests would need to involve comparisons using identical materials.

Predictive accuracy depends on the extent of basic paper tests performed. For a general product-use selection of paper, knowing only the cross-direction strength might be adequate. For papermaking process control studies, knowing strength and stiffness in both directions might be required.

To rank alternative tests of identical materials by accuracy, Eq. 16 should first be fitted to the data. If the experiment has been designed to generate both elastic and inelastic postbuckling failure, superior test methods will yield low confidence intervals for all three parameters of Eq. 16. If the confidence intervals are too large—that is, at least one parameter effectively equals zero—then Eq. 14 should next be fitted, followed by Eq. 15. With a poor combination of test methods, additional ECT strength beyond the critical load will not be discernible, and only Eq. 15 will yield low confidence intervals.

Conclusions

Postbuckling theory developed for metal plate structures has been applied to the microplate elements of corrugated fiberboard short columns to account for the large axial deformations at compression failure. The theory successfully predicts single-wall corrugated short column strength from paper properties determined in two cases using alternative testing methods. Short column strength was found to depend on paper compressive strength and on an overall microplate stiffness due to extensional and flexural paper properties and flute dimensions. Paper strength has the greatest effect on short column strength.

Although having less effect on short column strength than paper strength, paper stiffness determines the onset of localized buckling and the ability at short column failure to utilize the full paper strength of each component. For this reason, paper strength should not be used as the sole specification in maximizing fiberboard strength. Paper in a short column structure was found to achieve an average of about 80% of its inherent precorrugated strength, depending on stiffness.

The theory has been found to correct for the differences in paper properties that occur with using alternative measuring instruments. Therefore, paper tests and short column tests can be selected according to convenient methods. The results of the postbuckling analysis are bounded by the input values of dimensionless buckling stress and would apply to other papers within those bounds. The postbuckling theory is generalized for arbitrary structure shapes and can have further applications for double-wall and triple-wall corrugated and for discrete box structures. Software proposed (30) based on these methods can be written to calibrate a strength model to agree with a user's testing practices.

Literature cited

1. TAPPI Official Test Method T 818, TAPPI, Atlanta, 1987.
2. TAPPI Provisional Method T 826, TAPPI, Atlanta, 1986.
3. Koran, Z. and Kamdem, D. P., Tappi J. 72(6): 175(1989).
4. Stott, R., Tappi J. 71(1): 57(1988).
5. Koning, J. W., Jr., Tappi J. 71(10): 62(1988).
6. Uniform Classification Committee, Uniform Freight Classification 6000-C, Rule 41, Chicago, Ill., 1983.
7. TAPPI Official Test Method T 811, TAPPI, Atlanta, 1988.
8. Earl, G. F., Paperboard Packaging (Jan.): 48, 50, 52(1990).
9. Proposed Standard Specification for Corrugated Fiberboard, ASTM, Philadelphia, 1989.
10. Standard Test Method D 2808, ASTM, Philadelphia, 1984.
11. Testing, Compression Report 64, Proj. 1108-4, The Institute of Paper Chemistry, Appleton, Wis., 1957, p. 1.
12. Gunderson, D., APPITA 37(2): 137(1983).
13. Gerard, G., Tech. Note 3784, National Advisory Committee for Aeronautics, Washington, D.C., 1957.
14. Von Karman, T., Sechler, E.E., and Donnell, L.H., Transactions of the ASME 54(5): 53(1932).
15. McKee, R. C., Gander, J. W., and Wachutz, J. R., Paperboard Packaging 48(8): 149(1963).
16. Johnson, M. W., Jr., and Urbanik, T. J., Wood Fiber Sci. 19(2): 135(1987).
17. Johnson, M. W., Jr., and Urbanik, T. J., ASTM J. Composites Technology and Research 11(4): 121(1989).
18. Johnson, M. W., Jr., and Urbanik, T. J., J. Appl. Mech. 51: 146(1984).
19. Urbanik, T. J., Tappi 65(4): 104(1982).
20. "Emendation," Tappi 65(7): 114(1982).
21. Setterholm, V. C., Tappi 57(3): 164(1974).
22. Rosenthal, M. R., USDA Forest Serv. Res. Pap. FPL 287, Forest Prod. Lab., Madison, Wis., 1977.
23. Bormett, D. W., Boxboard Containers (Nov.): 30(1986).
24. The Institute of Paper Chemistry, Testing, Compression Report 85, Proj. 2695-3, 1967, p. 1.
25. TAPPI Official Test Method T 494, TAPPI, Atlanta, 1988.
26. TAPPI Official Test Method T 489, TAPPI, Atlanta, 1986.
27. Koning, J. W., Jr., Tappi J. 69(1): 74(1986).
28. Whitsitt, W. J. and Sprague, C. H., Tappi J. 70(2): 91(1987).
29. TAPPI Official Test Method T 411, TAPPI, Atlanta, 1984.
30. U.S. Dept. of Agriculture, Forest Service, Forest Prod. Lab., Commerce Business Daily, Sept. 25, 1989.

Received for review Nov. 10, 1989.

Accepted May 31,1990.